Supporting information

Insight into kinetics and mechanisms of AOT vesicle adsorption on silica in unfavorable conditions

*Julie WOLANIN [a], Loïc BARRÉ [a], Christine DALMAZZONE * [a], Didier FROT [a], Jacques JESTIN [b], Hubert PERROT [c], Daniela BAUER [a]*

[a] IFP Energies nouvelles, 1 et 4 avenue de Bois-Préau, 92852, Rueil Malmaison, France

[b] Laboratoire Léon Brillouin, CNRS-CEA, 91191 Gif-sur-Yvette, France

[c] Sorbonne Université, CNRS, Laboratoire Interfaces et Systèmes Electrochimiques, LISE, 75005 Paris, France

Contents

List of Figures

List of Tables

S1. Neutral pH: surface tension versus concentration plots

S1.1. Surface tension vs. concentration plots of AOT

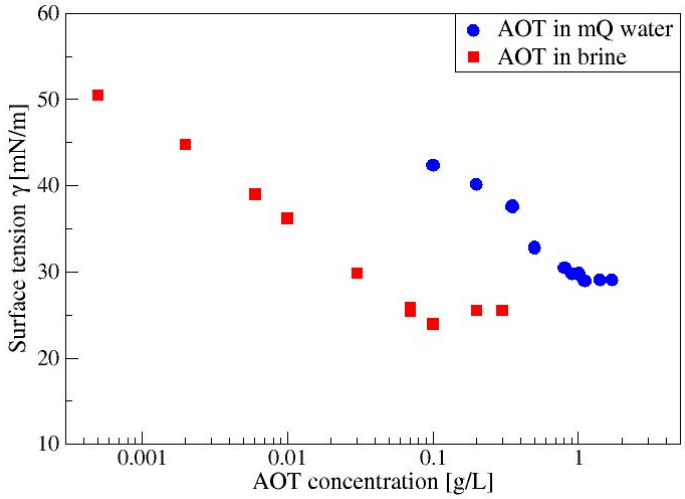

Figure S1: Surface tension versus AOT concentration plots (in mQ water and in brine solution)

S1.2. Comparison with the literature

We observe in Figure S2 that the slope of the SFT curves becomes steeper in the case of purified surfactants with EDTA and cationic exchange resin. The slopes of the curves obtained with our system are similar to those obtained with the commercial NaAOT by Li et *al*[1]. Our system (NaAOT in brine) shows characteristics features of an impure AOT: a shallow slope and the fact that γ is tending toward a value that is less than the expected 72 mN/m.

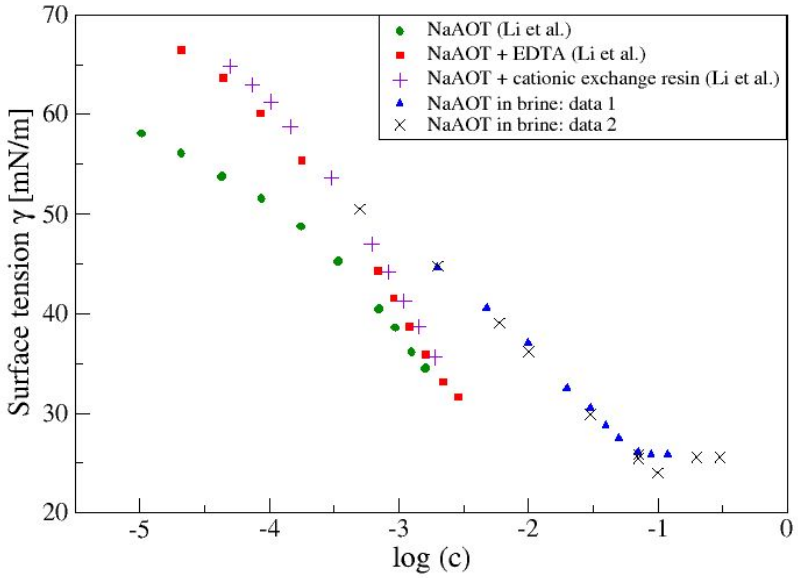

*Figure S2: Comparison of surface tension curves with the data obtained by Li et al.[1] (Adapted with permission from Langmuir **1997**, 13, 3681-3685. Copyright 2020 American Chemical Society). Two independent measurements of our AOT/brine system are presented.*

S2. Neutral pH: application of the Kelvin-Voigt model

For the neutral pH, quantitative information on the soft adsorbed layers can be obtained using the Kelvin-Voigt model[2] as the Sauerbrey model is not valid anymore ($\Delta D_n/n >> 2\text{x}10^{-6}$ and spreading of overtones). In the model presented by Voinova et *al.*[2], the adsorbed layer is represented by a single Voigt element, the quartz crystal is supposed to be purely elastic and the bulk solution to be purely viscous and Newtonian. Frequency and energy dissipation variations can be related to the film viscosity (η), shear modulus (μ), thickness (h), and density (ρ).

The use of this model is questionable since the thickness of the adsorbed layer is very small but a proposition is presented below and compared to the model presented for neutron reflectivity data. The Kelvin Voigt model was applied on the plateau values (step ③, between 2h35 and 2h48). To model our system, we have considered a three layers structure (Figure S3). The baseline solution (brine 15 g/L NaCl) was the semi-infinite Newtonian liquid (fixed parameters ρ_N= 1.01 g/cm^3 et η_N = 1.00 cP). Layer 1 (L_1) is the surfactant adsorbed layer (ρ_1, η_1, μ_1 and h_1). Layer 2 (L_2) is the AOT surfactant solution above the adsorbed layer (ρ_2, η_2, μ_2 and h_2) which is different from the Newtonian liquid (brine solution) due to the presence of AOT vesicles in solution. The densities of L_1 and L_2 were also set as an input parameter: ρ_1=1.1 g/cm^3 and ρ_2=1.01 g/cm^3.

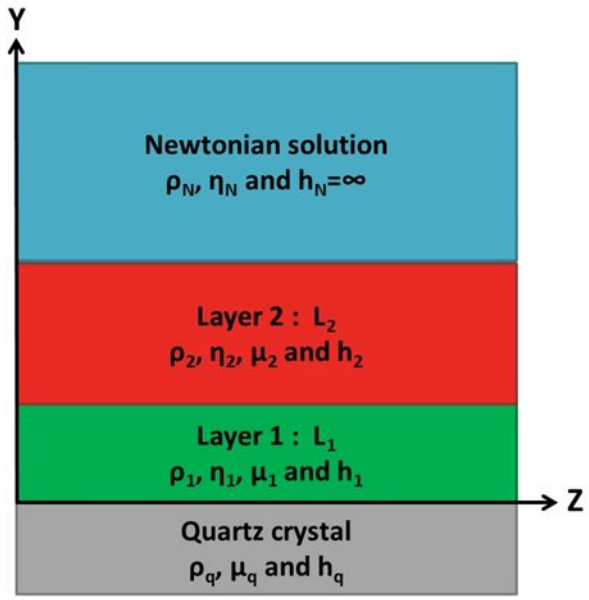

Figure S3: Application of the Kelvin-Voigt model for the neutral pH: a quartz crystal covered by two viscoelastic layers

The parameters obtained from the best fit of the experimental data are presented in Table S1. The thickness of L_2 (110 nm) is large compared to L_1's (8.5 m): therefore, L_2 characteristics may correspond to the AOT vesicular solution above the adsorbed layer L_1. Moreover, L_1 is much more viscous (2 cP) than L_2 (1.1 cP) due to the locally increased concentration of vesicles on the surface. For L_1 and L_2, we obtained $G''<G'$ staying for the fact that both layers are slightly rigid. However, μ_1 and μ_2 are lower than those found by Viitala et *al.*[3] when adsorbing phospholipidic vesicles onto a silica surface (~ 0.15 MPa). In this configuration, vesicle/surface interactions are stronger than in our case. The thickness of L_1 (8.5 nm) is of the same order of magnitude as that obtained from neutron reflectivity data (9.2 nm). Thus, the model is coherent, and data obtained with QCM-D are consistent with those of neutron reflectivity.

Table S1: Parameters calculated with the Kelvin-Voigt model for the neutral pH

	η [cP]	μ [Pa]	h [nm]
L_1	2.0 ± 0.04	(6.0 ± 0.2) x 10^5	8.5 ± 0.3
L_2	1.1 ± 0.01	1299 ± 299	110 ± 19

S3. Neutron reflectivity: second contrast measurement for the neutral pH

For the neutral pH, the reflectivity profile in a different contrast (AOT in a deuterated form and brine (H_2O/D_2O (0.595:0.405 in %w), called "CMSi" for contrast-matched water to silicon) was also obtained (Figure S4). In this case, we used a solvent that "matches" the silicon wafer, in order to highlight the surfactant adsorbed layer. The experimental data of the Figure S4 cannot be fitted with exactly the same 7-layer model presented in the publication. However, the models proposed at the two contrasts are quite similar, making it possible to give a unified proposition.

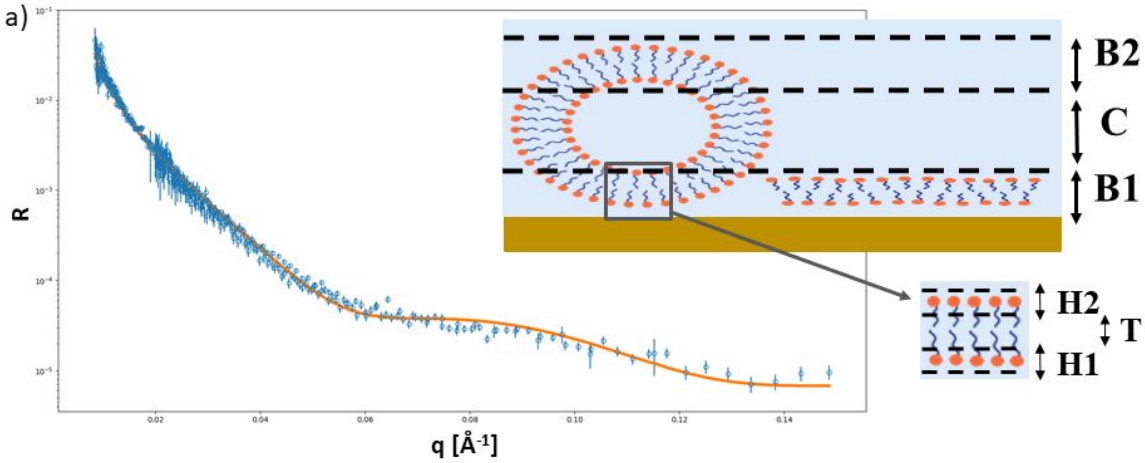

Figure S4: Reflectivity profile, fit and schematic diagram of the AOT adsorbed layer

In Figure S4, the two layers B1 and B2 are no longer symmetrical in terms of molecular composition (see Table S2). Since the bilayer B1 is more concentrated in surfactants, we assume that a small fraction of vesicles has ruptured to give an adsorbed layer composed of vesicles co-adsorbed with bilayer patches. The total thickness of the layer (7.6 nm) is lower than that found with the first contrast (9.2 nm) but both are of the same order of magnitude. The lower thickness obtained with the 2nd contrast can be explained by the presence of a less well-defined interface, adsorbed layer/bulk, (B2 containing much more water than B1, φ_{B2} ~0.8) making its characterization more difficult.

The two structural models have many similarities making it possible to characterize the structure of the adsorbed layer at neutral conditions. The observed differences between the two contrasts can be explained by experimental conditions that are not perfectly identical:

- a different silicon wafer was used for each contrast

- different AOT impurities related to the synthesis of the hydrogenated and deuterated forms (deuterated AOT ($C_{20}D_{34}H_3NaO_7S$) with a purity < 96% was purchased from Sigma Aldrich, product number 710652)

- a different protocol was used to obtain the vesicular solutions: for the 1st contrast; AOT was directly added into the brine solution while for the 2nd contrast the vesicular solution was prepared from a micellar solution. Indeed, the 50 mg deuterated AOT powder purchased from Sigma Aldrich was received in a 5 mL vial. Thus, to recover all the powder, it was diluted in pure D_2O (better solubility of AOT in mQ water than in brine solution).

- the size distributions of the vesicles obtained by DLS are slightly different due to isotopic substitution

Table S2: Parameters of the 7-layer model (2nd contrast)

	B1				**B2**		
	H1	**T**	**H2**	**C**	**H1**	**T**	**H2**
$\boldsymbol{d}$ **[nm]**	0.95	0.24	0.9	3.2	1.0	0.25	1.1
$\boldsymbol{\sigma}$ **[nm]**	0.2	0.1	0.4	1.7	0.3	0.1	0.7
$\boldsymbol{\varphi}$	0.62	0.09	0.5	0.96	0.83	0.3	0.75

S4. Neutral pH: adsorption of AOT under different conditions

S4.1. Adsorption of AOT in mQ water on silica

No adsorption was measured in mQ water (Figure S5) as also observed by Wang et *al.*[4]. If the adsorption process was essentially calcium driven, AOT would adsorb on silica even in mQ water.

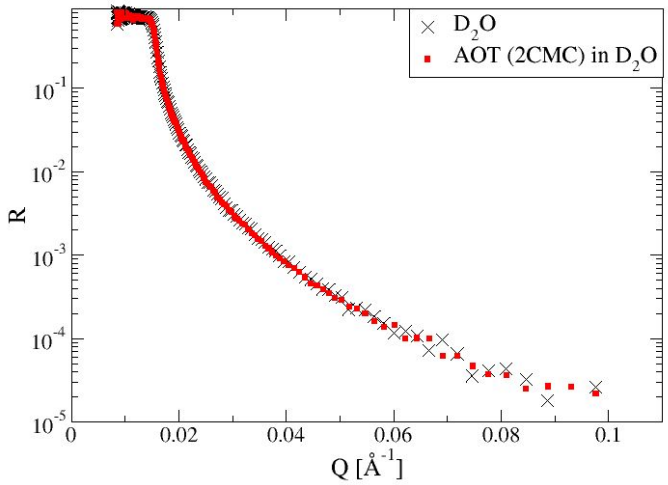

Figure S5: Reflectivity profiles of the bare silicon wafer (in contact with D_2O) and AOT surfactant in mQ water at 2CMC

S4.2. Adsorption of AOT below the CVC

The reflectivity profile obtained for the adsorption of AOT on silica at 0.6CVC is presented below. No adsorption was measured by neutron reflectivity experiments, probably because the adsorption is below the detection limit of the experiment.

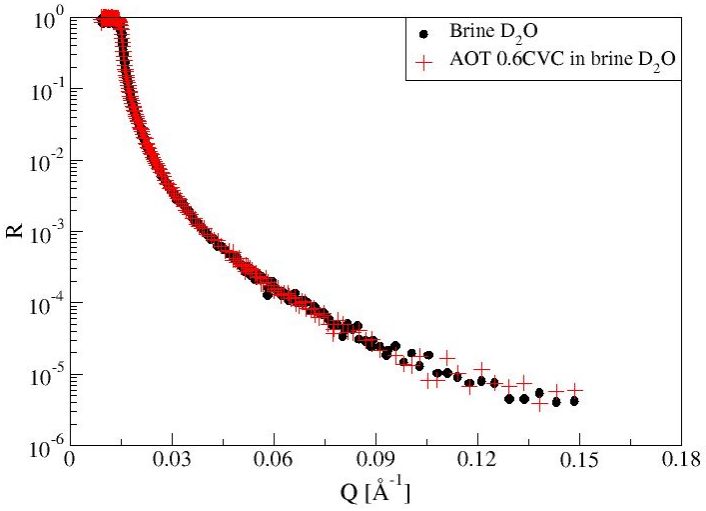

Figure S6: Neutron reflectivity: adsorption of hydrogenated AOT at 0.6CVC in deuterated brine on silica at neutral pH

The curves obtained with QCM-D experiments for the adsorption of AOT on silica below the CVC are presented in Figure S7. QCM-D curves show slight adsorption below the CVC attributed to monomers adsorption.

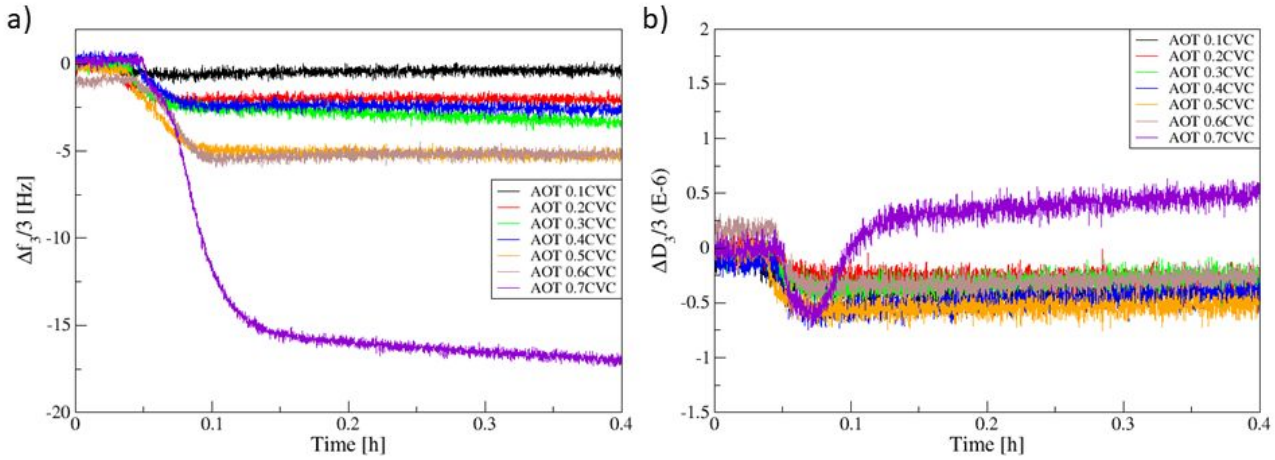

Figure S7: QCM-D: adsorption of AOT on silica at concentrations below the CVC

The comparison between the kinetics of AOT adsorption on silica below and above the CVC is presented below.

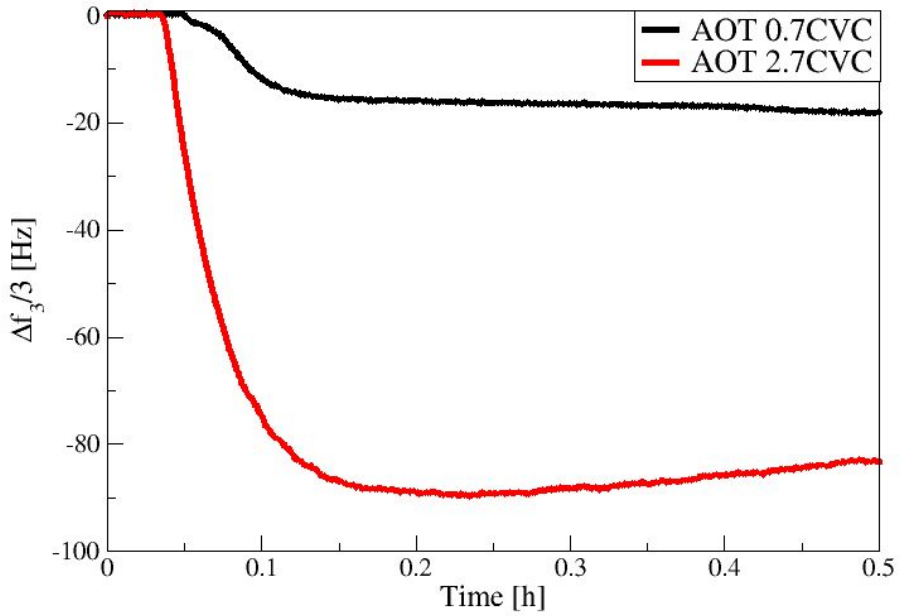

Figure S8: Adsorption kinetics of AOT in brine

Different kinetics are observed below and above the CVC. We measure a sharp increase in the initial adsorption rate at 2.7CVC. The difference of adsorption rates between 0.7CVC and 2.7CVC can be attributed to different adsorption mechanisms[5]. We suppose the adsorption of monomers below the CVC and of vesicles above the CVC.

S4.3. Adsorption of AOT above the CVC on alumina

The adsorption of AOT/brine system has been also investigated on alumina. The QCM-D curves are presented below. Results clearly demonstrated the direct adsorption of AOT monomers (monotonic curves) instead of vesicles. In this system, we have strong attractive electrostatic interactions. The curves are similar with no salt addition showing that the increased ionic strength has a negligible effect on this adsorption phenomena.

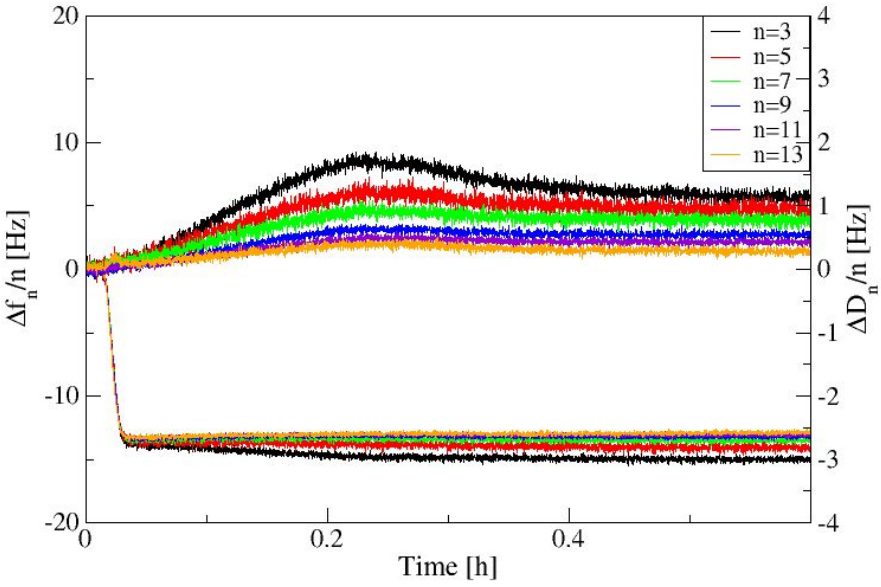

Figure S9: Adsorption of AOT at 1.3CVC on alumina at 20°C at intermediate pH

References

(1) Z. X. Li,J. R. Lu, and, and R. K. Thomas. Neutron Reflectivity Studies of the Adsorption of Aerosol-OT at the Air/Water Interface: The Surface Excess. *Langmuir* **1997**, *13*, 3681–3685.

(2) M. V. Voinova, M. Rodahl, M. Jonson and B. Kasemo. Viscoelastic Acoustic Response of Layered Polymer Films at Fluid-Solid Interfaces: Continuum Mechanics Approach. *Physica Scripta* **1999**, *Vol. 59*, 391–396.

(3) Viitala, T.; Hautala, J. T.; Vuorinen, J.; Wiedmer, S. K. Structure of anionic phospholipid coatings on silica by dissipative quartz crystal microbalance. *Langmuir* **2007**, *23 (2)*, 609–618.

(4) X. Wang, S. Y. Lee, K. Miller, R. Welbourn, I. Stocker, S. Clarke, M. Casford, P. Gutfreund and M. W. A. Skoda. Cation bridging studied by specular neutron reflection. *Langmuir* **2013**, *29 (18)*, 5520–5527.

(5) Velegol, S. B.; Fleming, B. D.; Biggs, S.; Wanless, E. J.; Tilton, R. D. Counterion Effects on Hexadecyltrimethylammonium Surfactant Adsorption and Self-Assembly on Silica. *Langmuir* **2000**, *16*, 2548–2556.